# Green's Function Retrieval and Marchenko Imaging in a Dissipative Acoustic Medium

Evert Slob*
*Delft University of Technology, 2628 CN Delft, The Netherlands*
(Received 5 August 2015; published 22 April 2016)

Single-sided Marchenko equations for Green's function construction and imaging relate the measured reflection response of a lossless heterogeneous medium to an acoustic wave field inside this medium. I derive two sets of single-sided Marchenko equations for the same purpose, each in a heterogeneous medium, with one medium being dissipative and the other a corresponding medium with negative dissipation. Double-sided scattering data of the dissipative medium are required as input to compute the surface reflection response in the corresponding medium with negative dissipation. I show that each set of single-sided Marchenko equations leads to Green's functions with a virtual receiver inside the medium: one exists inside the dissipative medium and one in the medium with negative dissipation. This forms the basis of imaging inside a dissipative heterogeneous medium. I relate the Green's functions to the reflection response inside each medium, from which the image can be constructed. I illustrate the method with a one-dimensional example that shows the image quality. The method has a potentially wide range of imaging applications where the material under test is accessible from two sides.

DOI: 10.1103/PhysRevLett.116.164301

*Introduction.*—Recently, a formulation has been found for obtaining the Green's function for a virtual receiver inside a 3D scattering acoustic medium from reflection data measured at one side of the medium [1]. This single-sided Marchenko equation was formulated by building on two developments in 1D problems and extending them to 3D. The first development was the recognition that solving the 1D Marchenko equation is equivalent to focusing an acoustic wave field inside the 1D medium, as demonstrated by Rose [2]. The second was finding that the 1D focusing wave field can be combined with its response to give the 1D Green's function, which was shown by Broggini and Snieder [3]. For virtual receivers in a horizontal plane inside the medium, the Green's functions of the upgoing and downgoing wave fields can be computed from the focusing wave field and the measured reflection response. The Green's functions can be used to obtain an image at the depth level of the virtual receiver location [4].

Dissipation of wave energy plays an important role in many scattering problems. In exploration geophysics, the rock-fluid interaction largely determines the dissipation properties. The dissipation can provide information on the rock permeability, fluid mobility, and fluid saturation that cannot be obtained from the velocity. This information is important for hydrocarbon exploration and production [5], and information obtained from rock samples is important for understanding field measurements [6]. Attenuation plays an important role in damage detection and characterization in nondestructive testing of laminated composites [7]. In medical imaging, attenuation and dispersion in biological tissue play an important role in diagnostic and therapeutic applications; while critically important for tissue characterization and treatment, it remains a challenge [8–11]. It is therefore useful to have a method to retrieve the Green's function inside a dissipative medium. In 1D the inverse scattering problem in a dissipative medium has been solved using Marchenko equations; the solution requires the full scattering matrix with infinite bandwidth as data [12,13].

Following the approach in [14], I show here that Green's functions for upgoing and downgoing wave fields can be retrieved using scattering data at two depth levels in a 3D heterogeneous and dissipative medium. I introduce the effectual medium as the medium that is the same as the physical medium, but with negative dissipation. For the dissipative medium, two coupled Marchenko equations are derived that use the single-sided reflection responses of both media to compute the focusing functions. Two similar coupled equations are derived for the effectual medium. I show that the reflection response of the effectual medium can be obtained from the double-sided measured reflection and transmission responses. I show how an image can be constructed from the computed upgoing and downgoing Green's functions and illustrate the method with a 1D numerical example.

*Green's functions representations.*—To derive 3D Green's functions representations I define the position vector of a spatial coordinate in a Cartesian reference frame as $\boldsymbol{x} = (x, y, z)$. The positive vertical axis points downward. Coordinates at a constant depth level $z_n$ are denoted $\boldsymbol{x}_n$ and the time coordinate is given by $t$. In the derivations I use three depth levels, i.e., the upper and lower boundaries at which measurements are available and an arbitrary depth level in between the upper and lower boundaries. The upper depth level is at $z_0$ and denoted $\partial\mathbb{D}_0$, the lower depth level is at $z_m$ and denoted $\partial\mathbb{D}_m$, the intermediate depth level at $z_i$ is denoted $\partial\mathbb{D}_i$, and $z_0 < z_i < z_m$. All heterogeneities are assumed to be located in the domain $\mathbb{D}$ defined between the outer depth levels, $\mathbb{D}_0$ and $\mathbb{D}_m$. I define the truncated domain as $\mathbb{D}_{0i} = \{(x, y) \in \mathbb{R}^2; z_0 < z < z_i\}$; the medium in

 

$\mathbb{D}_{0i}$ is called the truncated medium. Time and frequency domains can be interchanged by employing a Fourier transformation, for which I use $\hat{p}(\boldsymbol{x},\omega) = \int p(\boldsymbol{x},t)\times \exp(-j\omega t)dt$, where $j$ denotes the imaginary unit and $\omega$ denotes angular frequency. In the frequency domain, the medium for which measurements are available is characterized in $\mathbb{D}$ by frequency and position-dependent mass density $\hat{\rho}(\boldsymbol{x},\omega)$ and compressibility $\hat{\kappa}(\boldsymbol{x},\omega)$. The effectual medium is characterized in $\mathbb{D}$ by $\hat{\rho}^*(\boldsymbol{x},\omega)$ and $\hat{\kappa}^*(\boldsymbol{x},\omega)$, where the superscript $^*$ denotes complex conjugation, which signifies the negative dissipation properties of the medium. The upper half space $z < z_0$ and lower half space $z > z_m$ are homogeneous domains.

In the dissipative medium the focusing wave field can be decomposed into its upgoing $[\hat{f}_1^-(\boldsymbol{x}_0,\boldsymbol{x}_i',\omega)]$ and downgoing $[\hat{f}_1^+(\boldsymbol{x}_0,\boldsymbol{x}_i',\omega)]$ parts, in which $\boldsymbol{x}_0$ denotes the observation point and $\boldsymbol{x}_i'$ the focusing point. Similarly, the up- and downgoing parts of the Green's function observed at $\boldsymbol{x}_i$ and generated by a downgoing source at $\boldsymbol{x}_0''$ are denoted $\hat{G}^{\pm}(\boldsymbol{x}_i,\boldsymbol{x}_0'',\omega)$. The measured reflection response of the dissipative medium to the same source and measured at $\boldsymbol{x}_0$ is given by $\hat{R}(\boldsymbol{x}_0,\boldsymbol{x}_0'',\omega)$. These wave fields are depicted in Fig. 1, from which it can be seen that the focusing wave field is defined in the truncated medium whereas the Green's function and the reflection response are defined in the full medium. Similar definitions can be given for wave fields in the effectual medium: they are represented with an overbar; e.g., $\hat{\bar{R}}(\boldsymbol{x}_0,\boldsymbol{x}_0'',\omega)$ denotes the reflection response of the effectual medium. Wave fields that travel in the same domain can be related through the reciprocity theorem of the time-convolution type. The theorem is valid for a dissipative medium, and the Green's function representation is known as [4]

$$\int_{\partial\mathbb{D}_0} \hat{R}(\boldsymbol{x}_0,\boldsymbol{x}_0'',\omega)\hat{f}_1^+(\boldsymbol{x}_0,\boldsymbol{x}_i',\omega)d\boldsymbol{x}_0 = \hat{f}_1^-(\boldsymbol{x}_0'',\boldsymbol{x}_i',\omega) + \hat{G}^-(\boldsymbol{x}_i',\boldsymbol{x}_0'',\omega). \quad (1)$$

When the wave fields travel in the effectual medium, the result is easily understood to be

$$\int_{\partial\mathbb{D}_0} \hat{\bar{R}}(\boldsymbol{x}_0,\boldsymbol{x}_0'',\omega)\hat{\bar{f}}_1^+(\boldsymbol{x}_0,\boldsymbol{x}_i',\omega)d\boldsymbol{x}_0 = \hat{\bar{f}}_1^-(\boldsymbol{x}_0'',\boldsymbol{x}_i',\omega) + \hat{\bar{G}}^-(\boldsymbol{x}_i',\boldsymbol{x}_0'',\omega). \quad (2)$$

Later I will show how to obtain the reflection response of the effectual medium from the measured data. Equations (1) and (2) state that when the downgoing focusing wave field is sent into the medium, its response to the truncated medium is obtained together with a Green's function. The Green's function is the upgoing response at a virtual observation point $\boldsymbol{x}_i'$ to a downgoing impulsive wave sent into the medium at $\boldsymbol{x}_0''$.

For waves propagating in a dissipative medium, time reversal applies to an effectual medium such that it compensates in time reversal for the amplitude decay in forward propagation [15]. Therefore, wave fields in the dissipative medium can be related to wave fields in the effectual medium through the reciprocity theorem of the time-correlation type. The introduction of an effectual medium here not only accounts for losses in the medium, but also corrects for amplitude decay of evanescent waves. Corrections for exponential decay can only be done within the fidelity limits of the measured data. For this reason, the second Green's function representation known for lossless media requires a modification. When the focusing wave field travels in the dissipative medium, the Green's function and the reflection response must be taken in the effectual medium, and vice versa. This leads to the modified versions of the second Green's function representation in lossless media [4], given by

$$\int_{\partial\mathbb{D}_0} \hat{\bar{R}}(\boldsymbol{x}_0,\boldsymbol{x}_0'',\omega)[\hat{f}_1^-(\boldsymbol{x}_0,\boldsymbol{x}_i',\omega)]^* d\boldsymbol{x}_0 = [\hat{f}_1^+(\boldsymbol{x}_0'',\boldsymbol{x}_i',\omega)]^* - \hat{\bar{G}}^+(\boldsymbol{x}_i',\boldsymbol{x}_0'',\omega), \quad (3)$$

$$\int_{\partial\mathbb{D}_0} \hat{R}(\boldsymbol{x}_0,\boldsymbol{x}_0'',\omega)[\hat{\bar{f}}_1^-(\boldsymbol{x}_0,\boldsymbol{x}_i',\omega)]^* d\boldsymbol{x}_0 = [\hat{\bar{f}}_1^+(\boldsymbol{x}_0'',\boldsymbol{x}_i',\omega)]^* - \hat{G}^+(\boldsymbol{x}_i',\boldsymbol{x}_0'',\omega). \quad (4)$$

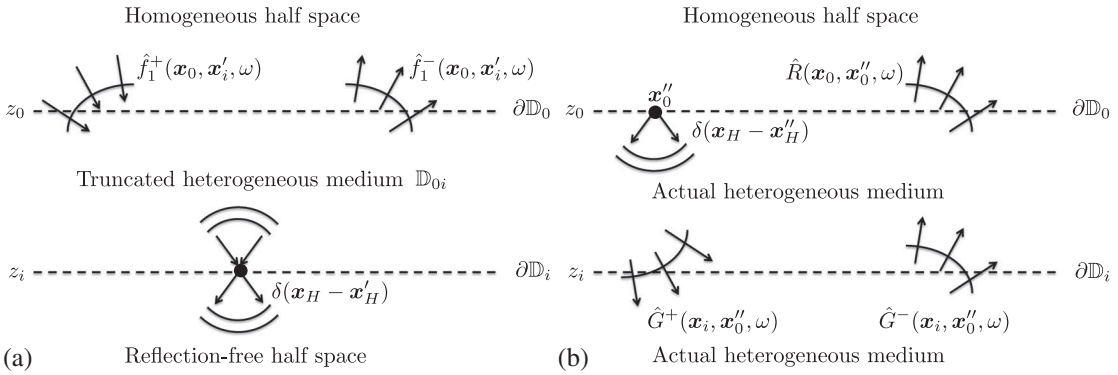


FIG. 1. (a) Down- and upgoing focusing functions, $\hat{f}_1^{\pm}(\boldsymbol{x}_0,\boldsymbol{x}_i',\omega)$, at $\partial\mathbb{D}_0$ and focusing at $\partial\mathbb{D}_i$. (b) Downgoing impulse and measurable reflection response, $\hat{R}(\boldsymbol{x}_0,\boldsymbol{x}_0'',\omega)$, at $\partial\mathbb{D}_0$ and Green's functions, $\hat{G}^{\pm}(\boldsymbol{x}_i,\boldsymbol{x}_0'',\omega)$, at $\partial\mathbb{D}_i$.

Equation (3) states that when the time-reversed upgoing focusing wave field in the truncated dissipative medium is sent into the effectual medium, the time-reversed downgoing focusing wave field in the truncated dissipative medium is obtained together with a Green's function. The Green's function is the downgoing response at a virtual point of observation $\boldsymbol{x}_i'$ to a downgoing impulsive wave sent into the effectual medium at $\boldsymbol{x}_0''$. Equation (4) can be interpreted in a similar way by interchanging the dissipative medium and the effectual medium. Equations (1) and (3) form one set of equations that can be solved in the time domain for the up- and downgoing parts of the focusing wave field in the dissipative medium if the reflection responses at $\partial\mathbb{D}_0$ are known in the dissipative and the effectual medium. Equations (2) and (4) form a similar set that can be solved using the same reflection responses. This is briefly explained below, because solving Marchenko equations and computing an image are well-known techniques.

*Marchenko-type equations and imaging.*—The procedure is the same for both sets; only the solution for the focusing wave field in the dissipative medium is described. Transforming Eqs. (1) and (3) to the time domain results in

$$G^-(\boldsymbol{x}_i',\boldsymbol{x}_0'',t) = -f_1^-(\boldsymbol{x}_0'',\boldsymbol{x}_i',t) + \int_{\partial\mathbb{D}_0}\int_{-\infty}^{t} R(\boldsymbol{x}_0,\boldsymbol{x}_0'',t-t') \times f_1^+(\boldsymbol{x}_0,\boldsymbol{x}_i',t')dt'd\boldsymbol{x}_0, \tag{5}$$

$$\bar{G}^+(\boldsymbol{x}_i',\boldsymbol{x}_0'',t) = f_1^+(x_0',\boldsymbol{x}_i',-t) - \int_{\partial\mathbb{D}_0}\int_{-\infty}^{t} \bar{R}(\boldsymbol{x}_0,\boldsymbol{x}_0'',t-t') \times f_1^-(\boldsymbol{x}_0,\boldsymbol{x}_i',-t')dt'd\boldsymbol{x}_0. \tag{6}$$

Both Green's functions in the left-hand sides of Eqs. (5) and (6) are zero for $t < t_d(\boldsymbol{x}_i',\boldsymbol{x}_0'')$, in which $t_d(\boldsymbol{x}_i',\boldsymbol{x}_0'')$ is the time instant of the first arrival. For $t < t_d(\boldsymbol{x}_i',\boldsymbol{x}_0'')$ the left-hand sides of Eqs. (5) and (6) are zero and the equations can be solved for the focusing wave field. By solving a similar system for $\bar{f}^{\pm}(\boldsymbol{x}_0'',\boldsymbol{x}_i',t)$, the up- and downgoing Green's functions in the dissipative medium can be computed from Eq. (5) and the time-domain equivalent of Eq. (4). The solution procedure is similar to the one given in [4], but there is an important difference. The initial estimate of $f_1^+[\boldsymbol{x}_0'',\boldsymbol{x}_i',-t_d(\boldsymbol{x}_0'',\boldsymbol{x}_i')]$ requires an estimate of the energy loss along the path from $\boldsymbol{x}_0''$ to $\boldsymbol{x}_i'$ at the time instant of the direct arrival that must be compensated for. Smooth loss and velocity models can be constructed from analyzing the two reflection responses. Once the Green's functions are obtained, the reflection response in the dissipative medium below $\partial\mathbb{D}_i$ can be obtained for $t > t_d(\boldsymbol{x}_i',\boldsymbol{x}_0'')$ from the mutual relation

$$G^-(\boldsymbol{x}_i',\boldsymbol{x}_0'',t) = \int_{\partial\mathbb{D}_i}\int_0^t R(\boldsymbol{x}_i',\boldsymbol{x}_i,t-t')G^+(\boldsymbol{x}_i,\boldsymbol{x}_0'',t')dt'd\boldsymbol{x}_i, \tag{7}$$

from which the image can be constructed by evaluating $R(\boldsymbol{x}_i,\boldsymbol{x}_i,0)$; other possibilities are given in [4]. It is possible to solve for the focusing wave field without making an estimate of the path loss from surface to the focusing point for the downgoing part of the focusing wavefield in the dissipative medium; this estimate, however, will be too weak. Using the same assumption for the initial estimate of the downgoing focusing wavefield in the effectual medium will result in a focusing wavefield that is too strong by the same amount. This will lead to similar errors in the Green's functions and, therefore, also in the reflection responses obtained from the Green's functions. A similar expression as Eq. (7) exists for $\bar{R}(\boldsymbol{x}_i,\boldsymbol{x}_i',t)$. In the frequency domain, the reflection response in the dissipative medium at the focus point should be equal to the one obtained from the effectual medium. This means that

$$\int_{\omega=-\infty}^{\infty}\hat{R}(\boldsymbol{x}_i,\boldsymbol{x}_i,\omega)d\omega = \int_{\omega=-\infty}^{\infty}\hat{R}(\boldsymbol{x}_i,\boldsymbol{x}_i,\omega)d\omega. \tag{8}$$

The deviation from this result is equal to twice the two-way path loss from surface to the focus point, with $\hat{R}$ being weak

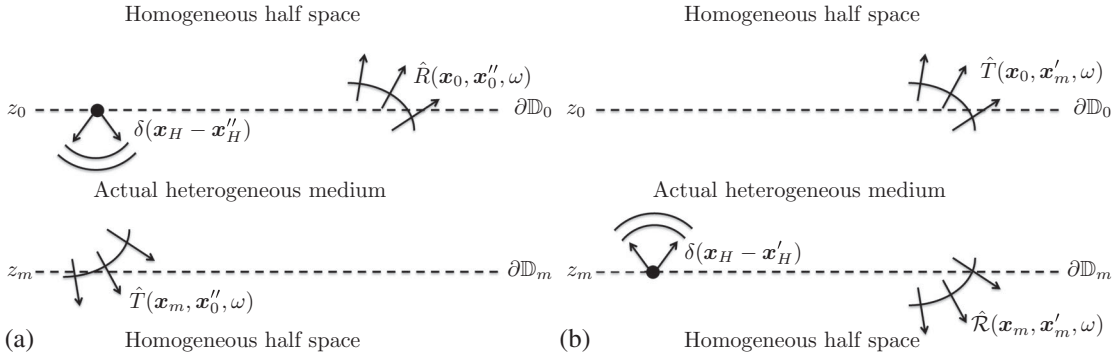


FIG. 2. (a) Downgoing impulse from the top at $\partial\mathbb{D}_0$ and measurable reflection, $\hat{R}(\boldsymbol{x}_0,\boldsymbol{x}_0'',\omega)$, and transmission, $\hat{T}(\boldsymbol{x}_m,\boldsymbol{x}_0'',\omega)$, responses at $\partial\mathbb{D}_0$ and $\partial\mathbb{D}_m$, respectively. (b) Upgoing impulse from the bottom at $\partial\mathbb{D}_m$ and measurable reflection, $\hat{\mathcal{R}}(\boldsymbol{x}_m,\boldsymbol{x}_m',\omega)$, and transmission, $\hat{T}(\boldsymbol{x}_0,\boldsymbol{x}_m',\omega)$, responses at $\partial\mathbb{D}_m$ and $\partial\mathbb{D}_0$, respectively.

and $\hat{\tilde{R}}$ being too strong by the same factor. This can be used to correct the amplitude of the image and is illustrated in the example below. Equation (8) will only result in a correction when the focus point is on a reflecting boundary; no correction is obtained in between reflectors. At such intermediate points there will be no image either, so it is of no concern.

*Retrieving the reflection response of an effectual medium.*—Figure 2 depicts the measurements that can be taken at two sides of a medium. Figure 2(a) shows that when a downgoing impulse is sent into the dissipative medium at $\boldsymbol{x}_0''$, its reflection response $\hat{R}(\boldsymbol{x}_0, \boldsymbol{x}_0'', \omega)$ can be recorded at $\boldsymbol{x}_0$ and its transmission response $\hat{T}(\boldsymbol{x}_m, \boldsymbol{x}_0'', \omega)$ at $\boldsymbol{x}_m$. Figure 2(b) shows that when an upgoing impulse is sent into the dissipative medium from below at $\boldsymbol{x}_m'$, its reflection response $\hat{\mathcal{R}}(\boldsymbol{x}_m, \boldsymbol{x}_m', \omega)$ can be recorded at $\boldsymbol{x}_m$ and its transmission response $\hat{T}(\boldsymbol{x}_0, \boldsymbol{x}_m', \omega)$ at $\boldsymbol{x}_0$. Similar results are obtained for the reflection and transmission responses in the effectual medium.

The double-sided reflection and transmission responses of the dissipative and the effectual medium can be put into a scattering matrix. In the operator sense, the scattering matrix of the effectual medium is the inverse of the complex conjugate of the scattering matrix operator of the dissipative medium. This leads to two equations for the reflection and transmission responses in the effectual medium in terms of the double-sided reflection and transmission responses in the dissipative medium, given by

$$\delta(\boldsymbol{x}_H' - \boldsymbol{x}_H'') - \int_{\partial\mathbb{D}_0} [\hat{R}(\boldsymbol{x}_0, \boldsymbol{x}_0', \omega)]^* \hat{\tilde{R}}(\boldsymbol{x}_0, \boldsymbol{x}_0'', \omega) d\boldsymbol{x}_0 = \int_{\partial\mathbb{D}_m} [\hat{T}(\boldsymbol{x}_m, \boldsymbol{x}_0', \omega)]^* \hat{\tilde{T}}(\boldsymbol{x}_m, \boldsymbol{x}_0'', \omega) d\boldsymbol{x}_m, \tag{9}$$

$$\int_{\partial\mathbb{D}_0} [\hat{T}(\boldsymbol{x}_0, \boldsymbol{x}_m', \omega)]^* \hat{\tilde{R}}(\boldsymbol{x}_0, \boldsymbol{x}_0'', \omega) d\boldsymbol{x}_0 = -\int_{\partial\mathbb{D}_m} [\hat{\mathcal{R}}(\boldsymbol{x}_m, \boldsymbol{x}_m', \omega)]^* \hat{\tilde{T}}(\boldsymbol{x}_m, \boldsymbol{x}_0'', \omega) d\boldsymbol{x}_m, \tag{10}$$

where $\hat{\tilde{T}}(\boldsymbol{x}_m, \boldsymbol{x}_0'', \omega)$ denotes the transmission response from a downgoing impulsive source at $\boldsymbol{x}_0''$ observed at $\boldsymbol{x}_m$ in the effectual medium. From these two equations the reflection and transmission responses in the effectual medium can be obtained. The reflection response is used in the Marchenko equations.

*Numerical example.*—The aim of the current method is to form an image of the inside of a sample under test given the measured reflection and transmission responses at two sides of the sample. Ideally the image amplitude should give the correct reflection amplitude of each interface between the layers. In that case, the reflection amplitudes can be used for further analysis to obtain the acoustic impedance of each layer. To illustrate the method I give a 1D example of a synthesized ultrasonic experiment on earth materials that could be carried out in a laboratory. The model mimics a layered medium with dissipation in mass density and compressibility in every layer using a Maxwell model. Figure 3 shows the values for the wave velocity, the mass density, and attenuation as a function of depth. The source emits a Ricker wavelet with 400-kHz center frequency. Because I use a Maxwell loss model, the attenuation is given in dB per wavelength ($\lambda_c$) at the center frequency of the source signal. Attenuation values around 0.3 dB/$\lambda$ represent consolidated sands or clays, values around 0.1 dB/$\lambda$ represent soft rocks, such as sandstones and siltstones, and values below 0.05 dB/$\lambda$ represent compacted rocks such as limestones, all common earth materials. I have computed the reflection and transmission responses at both sides of the layered medium. The source and receiver are 15 mm above the first interface for reflection measurements and a receiver is located at 20 mm below the bottom interface for the transmission measurements, cf. Fig. 2(a). For the reflection and transmission measurements with a source below the bottom interface, the same distances are used, cf. Fig. 2(b). From these measurements, the reflection response of the effectual medium is computed from Eqs. (9) and (10). The two reflection responses above the first interface are used to solve for the focusing wave fields at all time steps. The time of the first arrival is equal to half the measurement time. If the correct amplitude would be used in the initial estimate for the focusing wave field, the image would be perfect. Such an estimate is difficult to obtain from the data; therefore, it is more interesting to see what happens when no loss is assumed in the initial estimate of the focusing wave field.

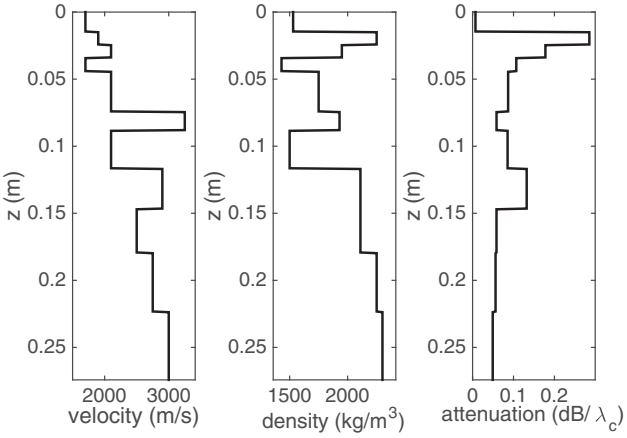


FIG. 3. Medium parameters of the model.

For this example, first the focusing wave fields are computed assuming a lossless medium as initial estimate for the focusing wave field. Then, the Green's functions are computed and the image is formed at each time step using Eq. (7) and keeping the value at zero time. This is done for the dissipative and the effectual medium. Then the procedure as described using Eq. (8) leads to the final image. Figure 4

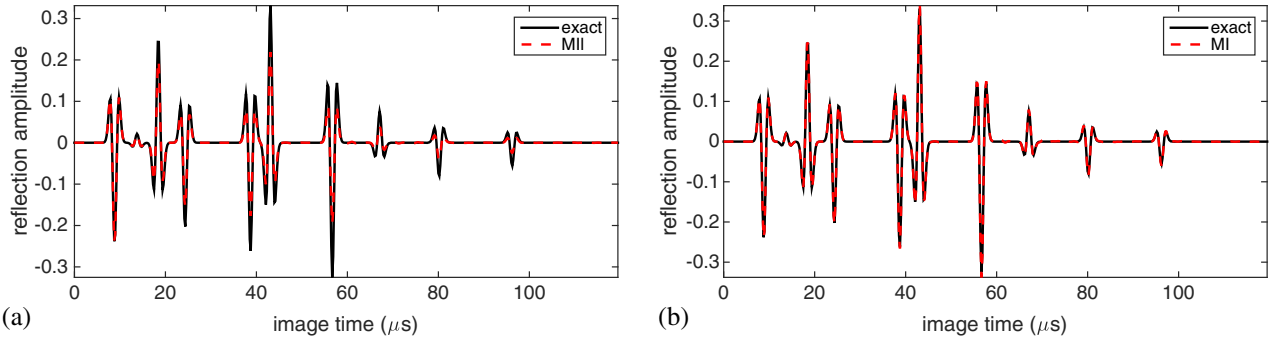


FIG. 4. Numerical example with the exact image convolved with the Ricker wavelet (exact, solid black) and results from the new scheme (dashed red) in (a) using Eq. (7) (MII) and (b) with amplitude correction using Eq. (8) (MI).

shows two Marchenko images (red dashed) together with the exact image convolved with the Ricker wavelet as a function of image time (solid black). Figure 4(a) shows the Marchenko image obtained using Eq. (7) for the dissipative medium and Fig. 4(b) shows the image obtained using the compensation procedure. Figure 4(a) shows that the scheme assuming no loss in the initial estimate for the focusing function produces a clean image but with incorrect amplitudes. The image in Fig. 4(b) is nearly perfect, with correct reflection amplitudes and almost free from ghost images due to multiple reflections in the data. This shows that amplitude correction is indeed possible using amplitude information of the images in the dissipative and effectual medium. To demonstrate the improvement over existing schemes, Fig. 5 shows two images, the conventional image (solid blue) obtained using the correct velocity model and the image obtained with the lossless Marchenko imaging scheme (dashed red) of [14]. The conventional imaging scheme does not apply any amplitude correction and images all multiples in the data as primary reflections. For this reason, the last three reflections that are clearly imaged in Fig. 4(b) cannot be distinguished from the multiples in the image of Fig. 5. The plot also shows that the image from the lossless Marchenko scheme has improved amplitudes, because of corrections from transmission effects, and the three multiples visible in the conventional image between 25 and 35 $\mu$s have

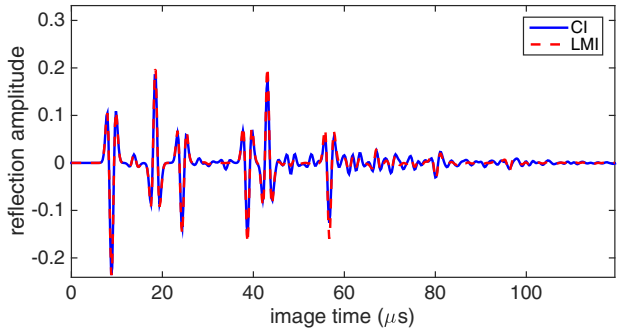


FIG. 5. Conventional image (CI, solid blue) and Marchenko image using the lossless scheme (LMI, dashed red).

been attenuated. The lossless Marchenko scheme does not correct for dissipation loss, which has two effects: the image amplitudes deteriorate with increasing image time and later multiples are imaged as primary reflection events, as can be seen in the plot for image times larger than 60 $\mu$s.

In terms of practical applications, similar experiments could be performed in the laboratory where both sides of a specimen would be available for measurements [6], or for medical purposes where measurements could be taken at two sides of the body. For such configurations, the new scheme is expected to perform better than existing methods. In 1D, no model information is necessary to carry out these steps. In 3D, some information is necessary to compute an estimate of the time instant of the first arrival [1].

*Conclusions.*—I have derived two independent sets of coupled single-sided Marchenko equations that can be solved for focusing wave fields inside a heterogeneous dissipative medium. These equations require as input the single-sided reflection responses of the dissipative medium and its corresponding effectual medium. The latter reflection response can be computed from reflection and transmission responses measured above and below the dissipative medium. To compute an image of the medium with the aid of the Green's functions pertaining to the dissipative medium, the focusing wave fields in both types of media need to be computed. The numerical example shows that the method is capable of accounting for the effect of realistic losses and can remove the effect of multiple scattered waves from the image. This was done without an estimate of the energy loss for the initial estimate of the focusing wave field. The current method has applications for nondestructive testing, medical imaging, and laboratory tests of real rocks that are important for hydrocarbon exploration; in all of these applications, the material under test is accessible from two sides. The method opens a new way to investigate how information on dissipative media contained in measured data can be used to produce a high-quality image, by accounting for propagation and dissipation in reflection and transmission as well as internal multiple scattering, with minimal *a priori* knowledge of the material properties.

I thank my colleague Kees Wapenaar for fruitful discussions on the topic and for carefully reading the manuscript. This Research was funded by Delft University of Technology.

*e.c.slob@tudelft.nl

[1] K. Wapenaar, F. Broggini, E. Slob, and R. Snieder, Three-Dimensional Single-Sided Marchenko Inverse Scattering, Data-Driven Focusing, Green's Function Retrieval, and Their Mutual Relations, Phys. Rev. Lett. **110**, 084301 (2013).

[2] J. H. Rose, Single-sided autofocusing of sound in layered materials, Inverse Probl. **18**, 1923 (2002).

[3] F. Broggini and R. Snieder, Connection of scattering principles: A visual and mathematical tour, Eur. J. Phys. **33**, 593 (2012).

[4] K. Wapenaar, J. Thorbecke, J. van der Neut, F. Broggini, E. Slob, and R. Snieder, Marchenko imaging, Geophysics **79**, WA39 (2014).

[5] B. Roy, L. Lines, M. Batzle, and J. Behura, Special section attenuation: Advances in analysis and estimation—introduction, Geophysics **79**, WBi (2014).

[6] G. Renaud, P.-Y. L. Bas, and P. A. Johnson, Revealing highly complex elastic nonlinear (anelastic) behavior of earth materials applying a new probe: Dynamic acoustoelastic testing, J. Geophys. Res: Solid Earth **117**, B06202 (2012).

[7] J. Dong, B. Kim, A. Locquet, P. McKeon, N. Declercq, and D. Citrin, Nondestructive evaluation of forced delamination in glass fiber-reinforced composites by terahertz and ultrasonic waves, Compos. Eng. **79**, 667 (2015).

[8] C. T. Barry, B. Millis, Z. Hah, R. A. Mooney, C. K. Ryan, D. J. Rubens, and K. J. Parker, Shear wave dispersion measures liver steatosis, Ultrasound Med. Biol. **38**, 175 (2012).

[9] G. Pinton, J.-F. Aubry, E. Bossy, M. Muller, M. Pernot, and M. Tanter, Attenuation, scattering, and absorption of ultrasound in the skull bone, Med. Phys. **39**, 299 (2012).

[10] R. Kruger, C. M. Kuzmiak, R. B. Lam, D. R. Reinecke, S. R. D. Rio, and D. Steed, Dedicated photoacoustic breast imaging, Med. Phys. **40**, 113301 (2013).

[11] J. Chen, Y. Gary, F. Marquet, Y. Hang, F. Camarena, and E. Konofagou, Radiation-force-based estimation of acoustic attenuation using harmonic motion imaging (HMI) in phantoms and in vitro livers before and after HIFU ablation, Phys. Med. Biol. **60**, 7499 (2015).

[12] V. H. Weston, On the inverse problem for a hyperbolic dispersive partial differential equation, J. Math. Phys. (N.Y.) **13**, 1952 (1972).

[13] M. Jaulent, Inverse scattering problems in absorbing media, J. Math. Phys. (N.Y.) **17**, 1351 (1976).

[14] E. Slob, K. Wapenaar, F. Broggini, and R. Snieder, Seismic reflector imaging using internal multiples with Marchenko-type equations, Geophysics **79**, S63 (2014).

[15] C. P. A. Wapenaar, M. W. P. Dillen, and J. T. Fokkema, Reciprocity theorems for electromagnetic or acoustic one-way wave fields in dissipative inhomogeneous media, Radio Sci. **36**, 851 (2001).